



Research Article

Light Hydrogen LENR in Copper Alloys

William H. McCarthy*

Shamrock Power, 2156 Old Middlefield Way, Mountain View, CA 94043, USA

Abstract

An example of Low Energy Nuclear Reaction (LENR) is demonstrated. A cell containing copper-boron alloy electrodes, infused with hydrogen at high temperature and moderate pressure, was tested. Calorimetry showing assumed nuclear energy well in excess of standard statistical requirements is reported. Equipment to detect far infrared emissions produced by these cells was built and is described. An electronic resonance method to reduce input is being developed to greatly improve efficiency. This should lead to a commercially viable energy source, with little or no environmental consequences. Some theoretical discussion is also given.

© 2019 ISCMNS. All rights reserved. ISSN 2227-3123

Keywords: Boron, Calorimetry, Capacitor, Copper, Hydrogen, Infrared, LENR, Resonance, Seebeck

1. Introduction

Low Energy Nuclear Reactions (LENR) produced in dilute copper alloys containing light hydrogen are described here. This system was selected because of the low cost of its constituents, ease of processing, and similarity to other, much more expensive, materials that have been extensively reported in the literature to produce nuclear heat. The focus here is on heat, with an excursion into thermal radiation, rather than on reaction products that are difficult and expensive to investigate.

A fundamental advantage, of LENR over other nuclear energy developments is the production of substantial power WITHOUT dangerous by-products. This research has been guided by the well-known nuclear reactions between the stable isotopes of hydrogen and the stable isotopes of boron and lithium that produce helium-four and more than 8 MeV of energy. Strong inter-particle forces in metals [as affected by solutes, dislocations, vacancies and the cloud of free electrons (in a quantum-mechanical environment)] must also be important in LENR.

2. Summary of Experimentation

The effort has three phases, each involving significantly different processes, complexity and instrumentation.

*Retired. E-mail: santander1bill@gmail.com.

(1) *Simple addition of hydrogen to a copper-based alloy*

Hydrogen was loaded into copper–lithium–boron alloys at elevated temperature (400–900°C) and pressure (about 10 atm.). The encapsulated specimens were quenched, and immediately inserted into a calorimeter to detect nuclear heat. That method had substantial experimental difficulty and showed little success. It is apparently too simple and has been discontinued.

(2) *Low- Q capacitors*

Cells containing hydrogenated copper–lithium–boron alloy electrodes separated by a liquid dielectric containing fine graphite particles have been tested. A vacuum-insulated Seebeck calorimeter was used. When the layers of copper alloy are alternately charged, electric currents are constrained to flow through the graphite particles at specific sites, resulting in microscopic variations of charge in the metal and localized electron flows. It seems that most, if not all, LENR observations involve charge dynamics. An example of anomalous heat from a low- Q capacitor is presented here. Results from another cell that had a cold worked electrode and different conductor/separator were posted at ICCF-18 [1]. That specimen showed about 9%, statistically significant, excess heat. Results from a control specimen, devoid of hydrogen, are indistinguishable from the corresponding joule calibration. Infrared images of electrodes producing anomalous heat by this method are being made.

(3) *Substantial reduction of input energy to produce useful power*

The low- Q capacitors are inherently inefficient because most of the input power is dissipated by resistance heating in the insulating layer between electrodes, and not available to stimulate nuclear reactions in the electrodes. Methods and apparatus to remedy this situation is being developed; they are described here.

3. Low- Q Capacitor

Electrodes containing less than one weight percent lithium and/or boron, as well as commercially pure copper have been tested. Hydrogenation of the electrodes is carried out in capsules pressurized to about 20 bar (300 psig) at 600–900°C. After 30 min or so, the capsule is water quenched. Dehydrogenation to prepare control electrodes is done by several vacuum (20 μ m Hg) anneals at about 700°C alternated with argon pressurization (20 bar).

Test cells are prepared from these copper alloy electrodes about 0.15 mm (0.005 in.) thick, 7 mm (0.25 in.) wide and 64 mm (2.5 in.) long. The electrodes are separated by thin gauze or thread saturated with a liquid or paste dielectric containing fine graphite particles, as illustrated in Fig. 1. They are stacked alternately to resemble capacitors. Electric conductance of the cells is controlled by varying the graphite concentration (2–12 vol.%). A fine dielectric powder (e.g. diatomaceous earth) is often added to separate graphite particles. These cells are thus poor (low- Q) capacitors with an inter-electrode resistance of three to twenty ohms. Their capacitance is a few nanofarads.

4. Calorimetry

The Seebeck calorimeter used here is based on a thermopile consisting of a series string of eight to ten Type-E thermocouple junction pairs. For this spider structure, the warmer junctions are cemented at the edges and between two strips of polycarbonate that form the base of the specimen carrier. The alternate cold junctions are cemented to similar polycarbonate strips attached to the body of the calorimeter, which is maintained at ambient temperature. Thin copper channels are cemented to the carrier polycarbonate on both sides, to stiffen the assembly and disperse any temperature gradients. The specimen is clamped to one side of the carrier with small brass screws and nuts. Thin rubber pads are included to prevent short circuits, without seriously affecting the sensitivity of the calorimeter. A joule heater is attached to the opposite side of the carrier, in as symmetrical a fashion as its geometry and that of the specimen allows. That electrical resistance heater consists of nichrome wire wrapped around a strip of polycarbonate and covered with a thin layer of silicone adhesive.

The thermocouple wires have three functions in this arrangement: They mechanically support the specimen/heater carrier, they signal the voltage corresponding to the temperature difference between carrier and ambient to measure the thermal power deposited on the carrier and they provide most of the thermal hurdle that maintains that temperature difference. The sensitivity of the calorimeter can be adjusted by selecting the diameter and length of thermocouple wires. A sketch of the power sensitive part of this calorimeter is shown in Fig. 2.

The spider is enclosed in a vacuum chamber as shown schematically in Fig. 3. That chamber has a clamshell design consisting principally of two copper half-cylinders, each brazed to steel quarter-spheres on the ends. The enclosure is mechanically pumped (about 20 $\mu\text{m Hg}$) to eliminate convection and greatly minimize gas-conduction heat transfer. There is some radiation cooling of the spider assembly. At the power levels used here (<650 mW), however, radiation can account for no more than one-quarter of the heat passed from the spider to the enclosure shell. It was found in practice that that level of thermal radiation is insufficient to produce detectable nonlinearity in the test results.

5. Testing

Cells are activated by direct current provided by a lead-acid battery. Thus, power factor concerns are eliminated. Current is controlled by a single-transistor power supply of the author's design and construction. The same Hewlett Packard Model 3445A voltmeter is used for all current and voltage (hence power) data. This instrument provides visual digital output with least count of one millivolt. The range of power levels used here is from about 50 to 600 mW. A four-wire hookup is used to connect the power supply to the specimen or joule heater, so that voltage drops in the leads do not affect the results.. The voltmeter has very high input impedance. A device is available to reverse automatically the specimen polarity. The typical reversal period of roughly ten minutes presents no power factor concern.

Voltage is measured directly. Current is measured by the voltage drop across standardized resistors. For any test

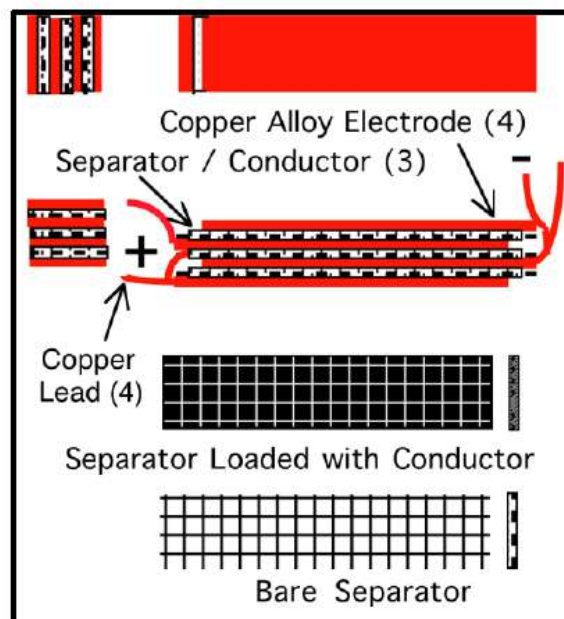


Figure 1. Cell schematic.

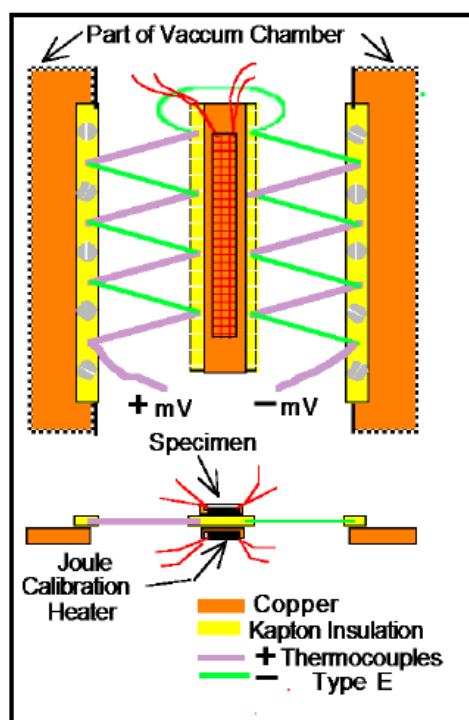


Figure 2. Seebeck calorimetry spider (heat sensor).

run, the same resistor(s) are used for both specimen and calibration heater. Joule heaters are designed to be fairly close in resistance to specimens. The standardized resistors are selected to be in the same range. Thereby, only one range of the voltmeter is normally used for joule and specimen readings (both current and voltage) over a moderate range of input power.

Thermopile output (dependent variable) is assessed using a Leeds & Northrup Model K-2 potentiometer. That 1960s era manually balanced Wheatstone bridge uses a calomel standard cell. It has a least count of $1 \mu\text{V}$. At a typical calibration minimum input of about 50 mW, the thermopile produces about one 1 mV. Precautions and other details of the instrumentation are discussed elsewhere [1] in much more detail.

The procedure is to power the cell or heater to some fairly arbitrary power level and wait perhaps an hour for thermal equilibrium, as shown by near constancy potentiometer readings from the K-2 instrument. Then typically three readings, separated by 5–10 min, are recorded. Input power is then adjusted, and/or input is switched between specimen (or polarity) and joule heater. To get some semblance of randomness, power levels are changed arbitrarily (not in up or down series, nor in order of power level). For operational efficiency, however, specimen and calibration will usually be switched at roughly the same power level. A set of the order of 50–100 equilibrium calibration and specimen data points is thus acquired over several days.

Readings are taken while power is stabilizing and the cell is coming to equilibrium. Those data are useful to assess calorimeter performance and to estimate total anomalous energy produced during a run. Only equilibrium data are used, however. So far, only manual data recording on paper has been employed, without automated data acquisition.

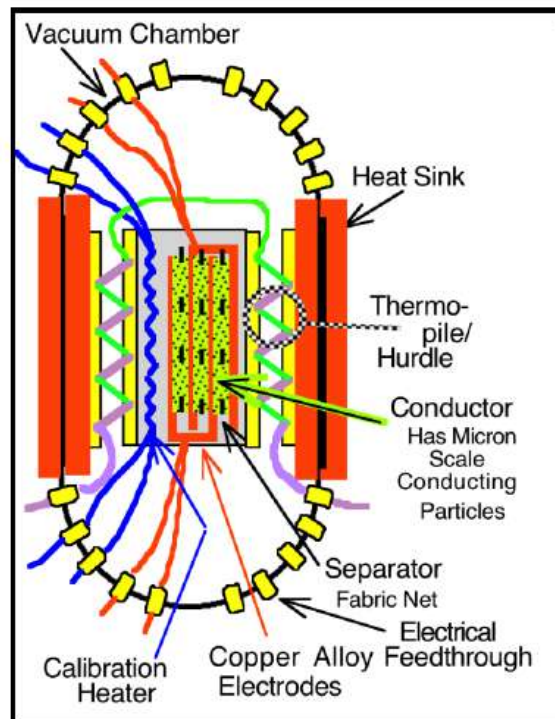


Figure 3. Calorimeter assembly.

The raw data are entered onto an Excel spreadsheet to calculate power, provide least-squares equations for calibration and specimen performance and to compile ancillary results. Data analysis and graphic displays are relied upon to define the performance of specimens and calibration heater, rather than trying to compare individual data points. Thus, the considerable trouble required for operation at precisely the same set of input levels for both heater and specimen measurements is avoided.

6. Example of Anomalous Heat

Some results from an active cell are given here. One electrode was a copper, 0.75 wt.% boron alloy hydrogenated at 820°C and 20 bar (300 psig) for 45 min, water quenched in capsule. The other electrode derived from a commercial copper tube. The separator was a layer of medical gauze about 25 μm (0.001 in.) thick. To make the conductor, it was saturated with a suspension containing nominally three micrometer (120 $\mu\text{in.}$) graphite particles in mechanical vacuum pump oil. Specimen resistance was about nine ohms to start. Figure 4 is a plot of thermopile output versus input power for that example.

Three-sigma statistical limits for the joule calibration data are defined by the band between the dashed green lines in Fig. 4. The 18 calibration data points are shown as green circles (in essentially isopower subsets of three). The green solid line is the least-squares fit of the joule calibration data. Red triangles and black squares indicate data points for the low- Q capacitor specimen. All data points, from the LENR cell, are well to the left (and above) the least-squares line of the calibration data. Above about 250 mW, the separations between the upper 3-sigma limit and the low- Q

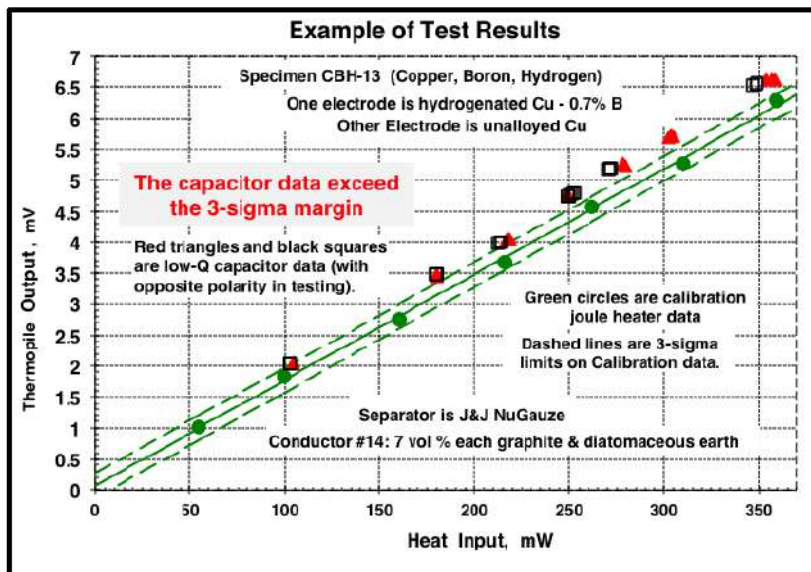


Figure 4. Test example showing anomalous heat.

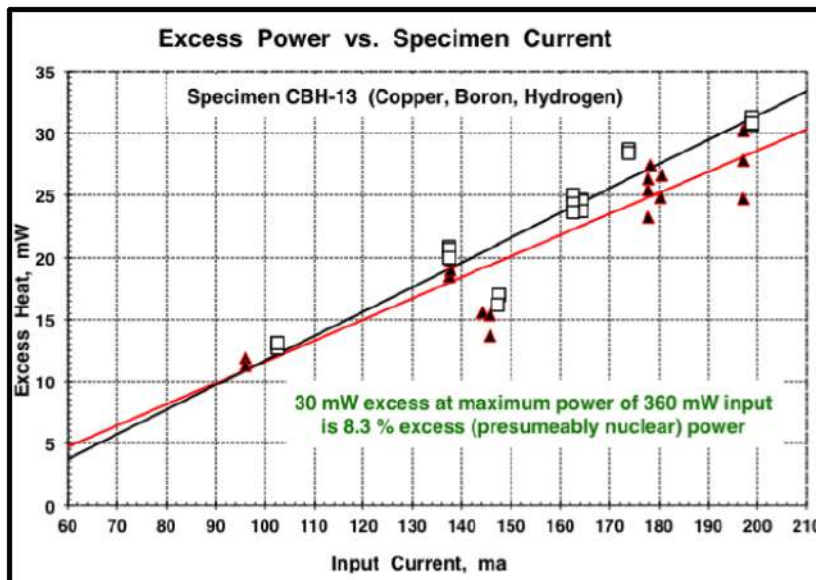


Figure 5. Anomalous power vs. input current from the data shown in Fig. 4.

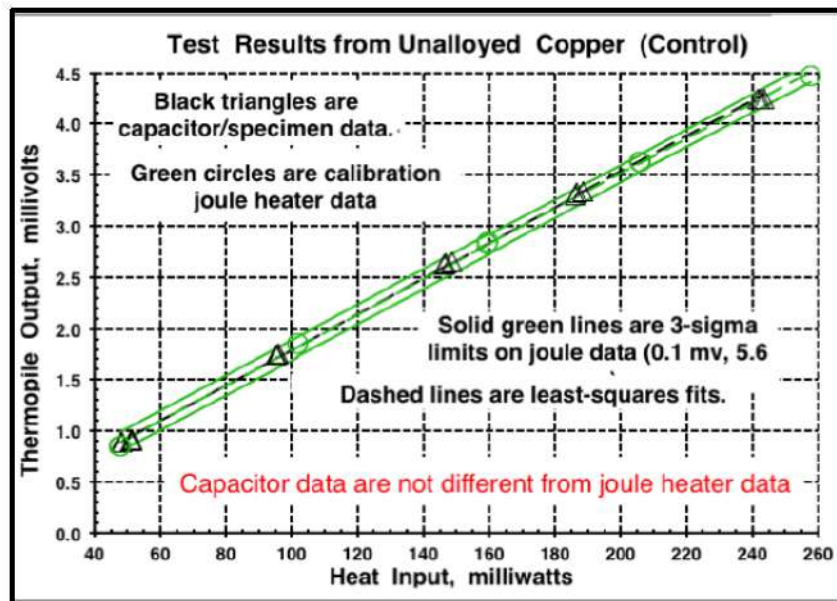


Figure 6. Test of dehydrogenated control electrodes.

data are roughly another 3-sigma amount. Therefore, the probability (assuming normal distribution and other standard statistical criteria) that the specimen and heater outputs are the same is much less than 0.3%.

Even though the low- Q capacitor results are substantially significant statistically, the magnitude of anomalous power (excess of output power over input) is small. In Fig. 5, anomalous power is plotted against input current, with red triangles for direct polarity and black squares for reverse. The assumed nuclear power reaches 30 mW at the maximum input of 360 mW. This is more than 8% of input, about one-half of which exceeds the three-sigma limit shown in the joule heater data. Nuclear power increases with input current at a roughly linear rate. Figures 4 and 5 show little difference between polarities.

7. Example of Vacuum Annealed Dehydrogenated Electrodes that Show No Anomalous Heat

A cell using commercial copper electrode materials subjected to dummy hydrogenation was prepared. Instead of high temperature pressurization with hydrogen, the electrode material was exposed at about 700°C to alternating vacuum and argon pressure. Results in the form of a plot of input power versus thermopile output are shown in Fig. 6. The joule calibration data are shown as green circles for the individual measurements (three per power level). The three-sigma band is defined by solid green lines. A dashed green line is the least-squares fit.

Specimen data are shown by black triangles. Least-squares fit for the capacitor is the dashed black line. In this case, there was no anomalous power because the dashed lines are indistinguishable, each from the other. This specimen behaved thermally exactly as did the joule heater.

The one-sided three-sigma limits for both joule heaters (Figs. 4 and 6), and for the dummy specimen are approximately equal (4.3–5.6 mW). Three-sigma limits for the active specimen are larger (6.6–15.3 mW) depending on polarity. The statistical “ r ” values from all five curve fits exceed 0.999.

8. A Working Hypothesis and Explanation

In researching a subject that lacks a widely accepted theory, it is helpful to create a working hypothesis of that subject's characteristics. Such a hypothesis facilitates consistency in decisions and minimizes thrashing about. One does not care if the hypothesis is precisely accurate; it can be abandoned or modified to correspond to developments. This working hypothesis is based on the well-known nuclear reactions between the stable isotopes of hydrogen and the stable isotopes of boron or lithium. These reactions produce helium-four *WITHOUT IONIZING RADIATION*. They create no dangerous emanations nor unstable nuclear residuals. The assumption is that hydrogen dissolved in some metals can react with specific light alloying elements (or tramp impurities) to produce helium and release more than 8 MeV of nuclear energy. Strong interatomic forces in metals, as affected by solutes, alloying particulates and the cloud of free electrons must also be important in LENR. This hypothesis readily explains LENR with both light and heavy hydrogen. A more complex process, involving sequential combination of four protons, is needed to explain the generation of helium from light hydrogen only.

The static forces inside metallic crystals seem insufficient trigger nuclear reactions. It is conjectured that significant motion of charges is required to cause protons (hydrogen ions: atoms stripped of their electrons) dissolved in a metal to move close enough to dissolved light element ions to fuse with the solutes which then break apart. Most, if not all, observations of LENR have taken place in dynamic systems having substantially moving electric charges. Obvious examples are acoustic bubble collapse and the plasma LENR techniques. Electron flow in the classic Pons–Fleischmann electrolytic LENR is disrupted by insulating gas bubbles on the cathode, also to cause considerable dynamism of the electronic distribution in the metal.

A proper metallurgical structure, and electric charges moving suitably therein, seems required. Edmund Storms [2] concept of a “hydroton” in a Nuclear Active Environment (NAE) seems especially cogent. The proposal there is that linear strings of oscillators are attached to micro-defects in the metal and vibrate coherently (as in a LASER). A photon is ejected simultaneously from each end of the hydroton dividing the very high energy of a nuclear reaction among a multitude of thermal oscillators to circumvent any need for hard emissions to release the energy. Dr. Storms looks to micro-cracks as the locations of these hydrotons; the current author believes dislocations are more likely sites. A suitable array of micro-cracks would be two dimensional, difficult to establish and maintain, but would be an explanation for the erratic occurrence of LENR. Dislocations, as sites for NAE, are ubiquitous, easy to control and they are curvilinear like the proposed string of oscillators.

It appears that Dr. Storms explanation for *light* hydrogen LENR on this basis is that two protons in a hydroton combine to form a deuteron which, in turn, reacts with another deuteron or a tritium ion to produce the observed result. See Table 11 in his book [2]. A direct process might be possible if a light-element ion (Li^{7+} or B^{11+}) were *part* of the hydroton. Table 1 lists such reactions for light hydrogen. (There are similar, considerably more energetic, reactions involving deuterium and the lighter isotopes of the same metals.)

Much longer, and higher power level, tests of these LENR cells should be run to get sufficient reaction so that isotopic changes can be measured. For instance, if an electrode containing natural boron and light hydrogen were to

Table 1. Some reactions of light hydrogen that produce no ionizing radiation.

${}^7\text{Li} + {}^1\text{H}$	\longrightarrow	$2\ {}^4\text{He}$	+17.3 MeV
${}^9\text{Be} + {}^1\text{H}$	\longrightarrow	$2\ {}^6\text{Li} + {}^4\text{He}$	+2.1 MeV
${}^{11}\text{B} + {}^1\text{H}$	\longrightarrow	$3\ {}^4\text{He}$	+8.7 MeV
${}^{11}\text{B} + {}^1\text{H}$	\longrightarrow	${}^{12}\text{C}$	+15.9 MeV

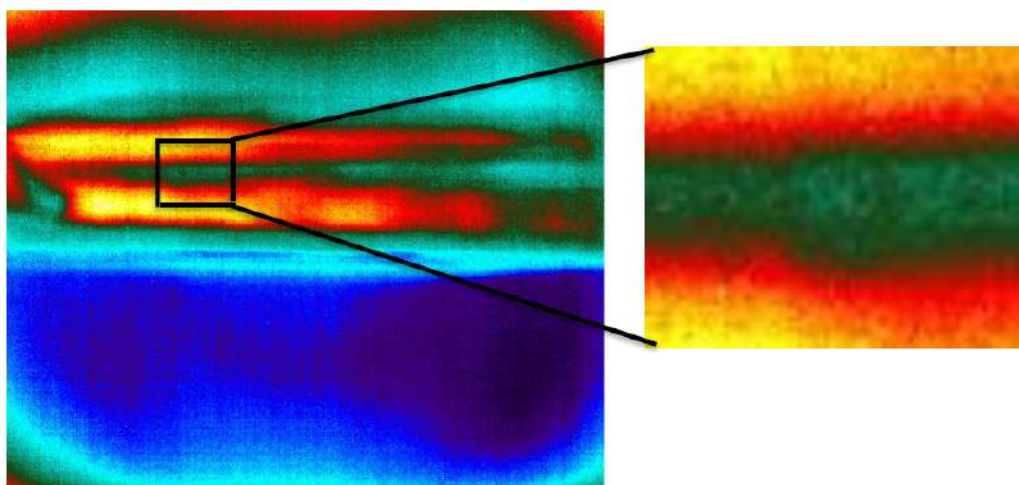


Figure 7. Preliminary infrared image.

be reacted sufficiently to show an increase in the B^{10}/B^{11} ratio, then the working hypothesis discussed above would be enhanced. It could be bolstered by an equivalent, or simultaneous, electrode containing deuterium instead, should that ratio decrease. A rough calculation shows that a cell like that discussed with Fig. 4, except using 0.25% by weight boron in copper electrodes, would have to be operated for more than 120 days at 30 mW nuclear heat to produce a change of 1% in the B^{10}/B^{11} ratio. The total nuclear energy evolved would also shine light on the nuclear chemistry.

9. Infrared Imaging of an LENR Cell

One impediment to the believability in LENR is the mystery of how a release of more than 8 MeV per nuclear event can be absorbed by heating a metal without producing any externally observable radiation. Such radiation would be in the X-ray or harder range (above about 1 keV (10^{16} Hz, wavelength less than 10 nm). If an active electrode could be imaged in the infrared through ultra violet range (10 μm –10 nm, 1 eV–1 keV) then substantial insight into the phenomenon should result. The longer the wavelength used in the imaging the better because shorter waves will degrade through phonon interaction.

A system has been set up around a digital camera with a vanadium oxide detection array that can image wavelengths from 7 to 14 μm . An evacuated Seebeck calorimeter was built along the previous design but containing a 5 mm (0.2 in.) thick zinc sulfide window that is transparent in the wavelength range of the camera. A test cell quite similar to the previous design was prepared except one somewhat transparent electrode was substituted. That electrode consists of a 2 mm (0.08 in.) thick plate of ZnS upon which a gold film has been deposited. The commercial gold film is a few μm thick and the mechanical application process resulted in many holes in the deposit. The previously used dielectrics inserted between electrodes (vacuum pump oil, vaseline) are opaque to infrared so glycerin was substituted. Ethylene glycol might have been used instead. The same fine graphite was suspended in the glycerin as previously, but in somewhat smaller concentration to minimally obstruct any infrared.

False-color images from the infrared camera focused on the active cell, as described above, are shown in Fig. 7. The larger picture on the left is approximately full size. The farther electrode of the cell is the greenish material between the red/yellow zones. The smaller image to the right is an electronic blow up of a portion of the other photo,

as indicated by the black lines. It barely resolves individual picture elements (pixels) which, in the 640×480 array, are about $150 \mu\text{m}$ (0.006 in.) square. So far, this work has not produced evidence of soft emanations produced by LENR. Image series in video show some twinkle, but not more from the cell than from other locations. Better transparent electrodes may improve the images.

The supplier of our ZnS makes only electronically intrinsic material. If n or p semiconducting ZnS could be found, the electrical conduction difficulty might be resolved. The n or p doping would have to be carefully controlled to minimize infrared opacity. Images focused on the edge of the cell should be made. Not only would this obviate the need for a transparent electrode, but it may be that the soft emanations are directed in the plane of the electrode. If some radiation came from the edge, rather than exiting the surface, much would be explained.

10. A Resonant Cell to Substantially Reduce Input Power while Maintaining Nuclear Output

The low- Q capacitor method described above is inherently inefficient because most of the input power goes to joule heat the conductor layer between electrodes. The input could be substantially reduced, at equivalent or greater current, by using a good capacitor made of the hydrogen-infused alloy, in an electronically resonant circuit.

Such a capacitor has been made from eleven plates of hydrogenated copper 0.7% boron alloy. The plates are each about 0.12 mm (0.005 in.) thick by 5 cm (2 in.) square. Silicone saturated baking parchment is used as the dielectric between alternately connected plates, to form the capacitor. After trials of some paints and plastic films, this parchment was selected because it is thin (about $25 \mu\text{m}$, 0.001 in.) is a good dielectric, useful above 200°C , and is fairly easy to apply. Teflon impregnated paper is available and equivalent except for its somewhat inferior dielectric constant. This capacitor, made with ten layers of parchment has a capacitance of about 12.5 nF and its resistance exceeds $20 \text{M}\Omega$. The total area of dielectric (about 250cm^2 , 40in.^2) is about 80 times the area of the dual-leaf low- Q capacitors previously used. If the 30 mW nuclear power of the best low- Q capacitors is proportionally maintained in a scaled-up resonant system, it would take nearly 24 h to heat 500 ml of ambient water to boiling.

That moderate power is, however, sufficient to obviate any need for sophisticated calorimetry. Accordingly, a system is being developed in which heated water can be drawn off periodically and be replaced by ambient temperature water. The power is determined by the amount and temperature of the water drawn off and the heating time. This is much like many of the classic Pons/Fleischmann experiments. That method should also allow for thermoelectric generators (TEG) to be inserted thermally between reservoirs of heated and ambient water. An objective is for the TEG to generate sufficient power to actuate the input electronics, at least after equilibrium has been reached. Then all batteries and external power sources could be removed and water will continue to be heated. That should put to rest all doubt about the validity of LENR. It will also show convincingly a way toward commercialization. No clear results have yet been produced. Frequency and wave form are being optimized using an external wave generator, without connecting an inductor to produce resonance. A search is being made for a commercial wave generator/amplifier, that will be efficient and well-matched to the optimized input signal.

11. Conclusions and Summary

Low Energy Nuclear Reaction (LENR) has again been demonstrated with an example provided. Copper alloys, infused with hydrogen at high temperature and moderate pressure, were used. A process for demonstrating this effect was outlined.

An explanation of some LENR observations was provided with a working hypothesis to organize further research. The assumptions are basically that hydrogen dissolved in some metals can react with specific light alloying elements to produce helium and more than 8 MeV of nuclear energy. *These reactions produce no dangerous products.* They require suitable metallurgical structures and electric charges moving therein. Modifications to a proposal by Storms [2]

involving the Nuclear Active Environment (NAE) and hydrotons were employed in this hypothesis. Equipment to image, at infrared wavelengths, cells producing anomalous energy has been assembled and was described here. An example of a photograph from that assembly was provided. The optical results have been inconclusive, so far. The effort continues. A system to radically improve LENR efficiency in copper alloys is being developed. It is expected that electronic resonance will result in devices to make LENR without any external energy source.

References

- [1] William H. McCarthy, Water-free replication of Pons–Fleischmann LENR, *J. Condensed Matter Nucl. Sci.* **15** (2015) 256–267.
- [2] Edmund Storms, *The Explanation of Low Energy Nuclear Reaction, An Examination of the Relationship between Observation and Explanation*, Infinite Energy Press, 2014, pp. 220–230.